

Inverse Evolution Layers: Physics-informed Regularizers for Deep Neural Networks

Chaoyu Liu^{1,*}, Zhonghua Qiao¹, Chao Li^{2,3}, Carola-Bibiane Schönlieb^{3,†}

¹ Department of Applied Mathematics, The Hong Kong Polytechnic University

² School of Science and Engineering & School of Medicine, University of Dundee

³ Department of Applied Mathematics and Theoretical Physics, University of Cambridge

`polyucy.liu@connect.polyu.hk; zhonghua.qiao@polyu.edu.hk; c1647@cam.ac.uk;`
`cbs31@cam.ac.uk`

Abstract

This paper proposes a novel approach to integrating partial differential equation (PDE)-based evolution models into neural networks through a new type of regularization. Specifically, we propose inverse evolution layers (IELs) based on evolution equations. These layers can achieve specific regularization objectives and endow neural networks' outputs with corresponding properties of the evolution models. Moreover, IELs are straightforward to construct and implement, and can be easily designed for various physical evolutions and neural networks. Additionally, the design process for these layers can provide neural networks with intuitive and mathematical interpretability, thus enhancing the transparency and explainability of the approach. To demonstrate the effectiveness, efficiency, and simplicity of our approach, we present an example of endowing semantic segmentation models with the smoothness property based on the heat diffusion model. To achieve this goal, we design heat-diffusion IELs and apply them to address the challenge of semantic segmentation with noisy labels. The experimental results demonstrate that the heat-diffusion IELs can effectively mitigate the overfitting problem caused by noisy labels.

1 Introduction

In recent years, deep learning has made a profound impact on many image processing tasks such as classification, segmentation and inpainting [2, 4, 12, 15]. Compared to conventional mathematical models based on partial differential equations (PDEs), deep neural networks can extract shallow and deep features from large-scale training datasets, enabling them to outperform the PDE-based methods on many image processing tasks when given sufficient data. However, it can be challenging to mathematically analyze the outputs of neural networks and regulate them to exhibit desired properties. In contrast, PDE-based methods have a strong theoretical foundation and are well-established in the field of mathematics and physics. This makes it easier to analyze and understand the behavior of these models, as well as provide theoretical guarantees on the solutions. Many PDE-based models have been extended to image processing tasks, achieving remarkable success [1, 5, 21, 26]. The results obtained from these models can be guaranteed to have certain desirable properties under mathematical analysis. For example, in [16], Liu *et al.* propose a PDE-based model by introducing phase field models and corresponding numerical schemes for image segmentation. The introduce of the phase field model enable the proposed model to exhibit strong robustness to noise. Therefore, there is a meaningful research opportunity to establish a bridge between

^{*}First author

[†]Corresponding author

traditional mathematical models and data-driven models and integrate powerful mathematical properties and tools into data-driven models.

There have been many studies on connections between partial differential equations and neural networks. In [30], Weinan *et al.* provided an explicit exposition of the connection between neural networks including the ultradeep ResNet [14] and dynamical systems. Subsequent research by Lu *et al.* [18] shows that many effective networks can be seen as different numerical discretizations of differential equations. Instead of explaining through discretized differential equation, Chen *et al.* [7] proposed a novel approach whereby a neural network is employed to parameterize the derivative of the hidden state with respect to a continuous time variable.

In addition to identifying the similarities between mathematical models and neural networks, many efforts have been made to integrating PDE-based models into neural networks. The most direct approach to achieving this objective is to add loss functions derived from various PDE models to regularize the outputs [8]. However, this method can cause intractable problems including gradient explosion during the training process when the added loss function lacks good derivative properties. Additionally, the added loss makes no contribution to the forward propagation during training or prediction. Recently, Liu *et al.* [17] proposed a novel method of adding loss by integrating spatial regularization into the constrained optimization problem generalized from the softmax activation function. This approach enables the loss to affect the forward propagation. However, this method may significantly increase the computation cost during training since it requires solving an optimization problem during each forward propagation.

In addition to loss-inserting methods, researchers have attempted to modify the architecture of neural networks to enhance their interpretability. For example, Chen *et al.* [9] developed a neural network for image restoration by parameterizing a reaction-diffusion process derived from conventional PDE-based image restoration models. Similar techniques that employ convolutional neural networks (CNNs) to learn parameters in active contour models can be found in [20, 10, 13]. In [19], Lunz *et al.* combine the neural networks with variational models for inverse problems by using a neural network to learn regularizers in the models. Ruthotto *et al.* [27] imparted mathemat-

ical properties of different types of PDEs by imposing certain constraints on layers. Raissi *et al.* [24] proposed Physics-Informed Neural Networks (PINNs) by approximating differential operators with automatic differentiation and imposing two loss functions for equations and boundary conditions to a neural network to enforce it behave as given partial differential equations. Although the interpretability of these networks has significantly improved, their performance and learning ability could be limited by the specified architecture or constraints. Moreover, the specified architecture and constraints make it challenging to find an optimal balance between interpretability and learning ability. Consequently, their specified architectures and constraints limit their applicability to a particular type of problem and make them unsuitable for improving other popular and advanced neural networks. For instance, PINNs have demonstrated efficacy in solving partial differential equations; however, their applicability to image processing tasks presents a significant challenge.

In this paper, we propose a novel method to integrate PDE models into a given neural network by adding layers derived from the inverse processes of corresponding evolution equations. These layers enable the neural network outputs to possess the desired properties of the solutions of the evolutions. Our proposed method differs from traditional loss-inserting techniques in that it has stronger interpretability and affects both forward and backward propagation during training. In addition, it does not suffer from gradient-related issues during the backward propagation stage. Furthermore, it also allows for convenient trade-offs between desired properties and neural network performance through adjustment of the evolution time.

The main contributions of this work are:

1. We propose a novel and straightforward framework for integrating PDE-based mathematical models into neural networks during training. This framework can be easily implemented and does not require any additional learning parameters. More importantly, it has strong generalizability and is applicable to a wide range of neural networks. In addition, our framework preserves the learning capabilities of the given neural networks as it does not alter their original structure or impose any constraints on them.

2. We develop the inverse evolution layers (IELs), which are derived from the inverse processes of the evolution equations in mathematical models. These layers have good interpretability and can act as regularizations by amplifying undesired properties of neural networks, thus compelling the neural networks’ outputs to possess the desired properties during training.

3. We introduce heat-diffusion IELs and evaluate their performance on several semantic segmentation models on datasets with normal labels and noisy labels. Experimental results demonstrate the effectiveness of our proposed approach.

The rest of this paper is organized as follows. In section 2, we provide a comprehensive description of the inverse evolution layers and the generalized neural network architecture with these layers, along with an explanation of how these layers can be utilized to regularize neural networks. In section 3, we present an example that employs heat-diffusion inverse evolution layers to address the issue of semantic segmentation with noisy labels. The experiment results show that our heat-diffusion IELs can significantly inhibit the networks’ noise overfitting issue. In section 4, we summarize the main contributions and findings of our work, and discuss potential avenues for future research.

2 Neural Networks with Inverse Evolution Layers

2.1 Inverse Evolution Layers

In this section, we introduce the inverse evolution layers (IELs) which play a pivotal role in our framework for integrating specific characteristics of mathematical models into neural networks.

In physics, evolution processes can be modelled by partial differential equations that vary over time. For instance, diffusion processes can be modelled by the diffusion equations [23, 29]. Additionally, advection–diffusion–reaction systems can be depicted through

advection–diffusion–reaction equations [22]. The solutions of these processes inherently possess favorable properties. For example, the solution to a diffusion process will have good smoothness. Rather than enhancing these desirable properties, we aim to develop layers that amplify opposing unfavorable properties. To achieve this goal, we first consider a general form of the partial differential equations of forward evolutions

$$u_t = \mathcal{F}(u), t \in [0, T], \quad (1)$$

where $u = u(t, x)$ denotes the analytical solution of an evolution, and \mathcal{F} refers to a combination of linear and nonlinear differential operators which may include a variety of gradient operators.

Using powerful tools in numerical mathematics, one can efficiently solve these PDEs and determine the values of variables at any time in the evolution. For example, if solving the general partial differential equation by a simple explicit forward Euler’s formula for temporal discretization and a finite difference scheme for spatial discretization, we can obtain the following discrete numerical scheme

$$\frac{u_{t+1} - u_t}{\Delta t} = F(u_t). \quad (2)$$

Here u_t and u_{t+1} respectively denote the solution at time T_t and T_{t+1} , where $T_{t+1} - T_t = \Delta t$. F represents finite difference approximations of \mathcal{F} , and $F(u_t)$ can be conceptualized as a combination of convolutions of u with designated filters.

We rewrite equation (2) as follows

$$u_{t+1} = u_t + \Delta t * F(u_t). \quad (3)$$

The above equation (3) demonstrates that once the precise value of u_t is known, the value of u_{t+1} can be determined. Moreover, given u_0 , it is possible to obtain a numerical solution at any time by iteratively applying this equation.

Based on the equation (3), we propose inverse evolution layers. Instead of solving evolutions in a forward manner, these layers are utilized to numerically simulate the inverse process of evolutions. From the equation (3), we can see that u_{t+1} is calculated by adding the term $\Delta t * F(u_t)$ to u_t . Therefore, a natural way to obtain the simulation of the inverse evolution is to replace the “+” with “-”. On this basis, we introduce the concept of inverse evolution layers. The construction of an inverse

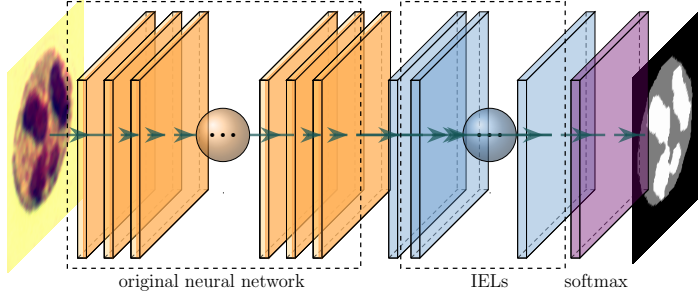


Figure 1: The architecture of neural networks with IELs. From left to right: input, original neural networks, (inverse evolution layers) IELs, softmax layer and final output. The original neural network can be any kind of neural networks. The IELs behave like a bad property amplifier. During training, the IELs will be activated while in prediction, they will be deactivated.

evolution layer is quite straightforward: we design a layer such that, given an input u , its output is

$$L(u) = u - \Delta t * F(u). \quad (4)$$

From equation (4), we can see that the inverse layer involves no learning parameters. In contrast to forward evolution, the inverse evolution layers are expected to amplify certain undesired properties, making them suitable for use in neural networks as a form of regularization.

2.2 The Architecture of Neural Networks plus Inverse Evolution Layers

Given a neural network, the way we incorporate inverse evolution layers is to add them to the output of the network before computing the loss function, as depicted in Figure 1. In our framework, we will activate the inverse evolution layers during training, while during the evaluation and prediction we will deactivate the inverse evolution layers.

As previously mentioned, inverse evolution layers are designed to magnify undesirable properties and increase the inconsistency with the corresponding forward physical process. For example, as the solution of the heat diffusion process is typically smooth, the corresponding inverse evolution layers will accentuate the roughness of

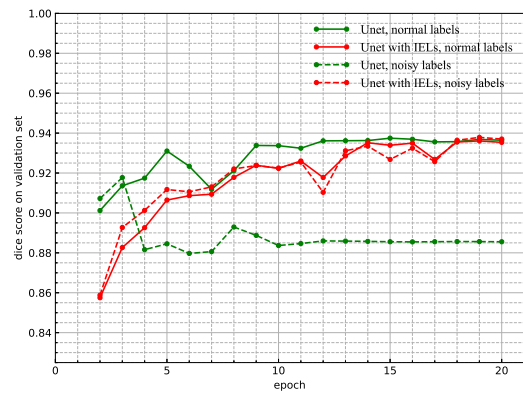


Figure 2: Dice score on the validation set of White Blood Cell (WBC) dataset based on Unet [25] and Unet with heat-diffusion IELs. The results of Unet and Unet with heat-diffusion IELs are highlighted by green lines and red lines, respectively. The results on normal labels and noisy labels are marked by solid lines and dotted lines, respectively.

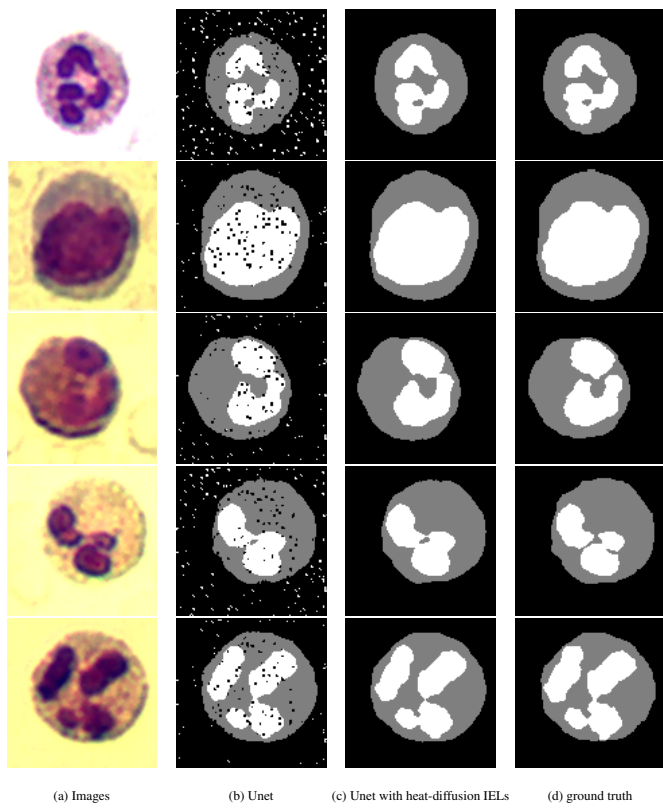


Figure 3: Comparison between Unet [25] and Unet with heat-diffusion IELs on White Blood Cell (WBC) dataset with noisy labels. (a) and (d) are the original images and the corresponding ground truth, respectively. (b) and (c) exhibit the segmentation results of the original Unet and Unet with heat-diffusion IELs, respectively.

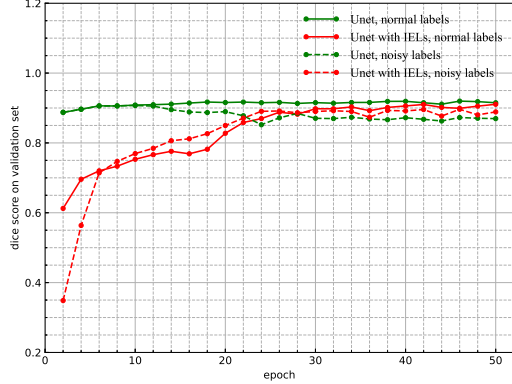


Figure 4: Dice score on the validation set of 2018 Data Science Bowl (DSB) dataset based on Unet [25] and Unet with heat-diffusion IELs. The results of Unet and Unet with heat-diffusion IELs are highlighted by green lines and red lines, respectively. The results on normal labels and noisy labels are marked by solid lines and dotted lines, respectively.

their inputs. Consequently, if the input to the inverse evolution layers, *i.e.* the output of the neural network, contains noise, the noise will be amplified after passing through the IELs.

Due to the specialized construction of the IELs, it can be anticipated that during the training phase, the undesired characteristics of the neural network’s outputs will be amplified after passing through the IELs. Thus, the IELs can serve as a form of regularization by penalizing the neural network to generate outputs that exhibit undesirable properties with much less frequency.

3 Diffusion IELs

3.1 Drivation of Diffusion IELs

In this section, we present a simple example by developing inverse evolution layers based on the heat diffusion equation. As the solution to the heat diffusion process is typically smooth, we can expect that the heat-diffusion IELs can effectively prevent neural networks from over-

neural networks	datasets	Δt	the number of IELs
Unet	WBC	0.1	20
	2018 DSB	0.1	30
DeepLabV3+	Cityscapes	0.1	35
HRNetV2-W48	Cityscapes	0.1	30

Table 1: IELs configurations for different neural networks on different datasets.

fitting noise in images.

The heat diffusion equation is formulated as

$$u_t = \Delta u, t \in [0, T]. \quad (5)$$

According to equation (4), we can construct IELs through the following formula

$$L(u) = u - \Delta t * F_\Delta(u), \quad (6)$$

where F_Δ , the finite difference approximation of Δ , can be depicted by the following 3×3 filter,

$$\begin{bmatrix} 0 & 1 & 0 \\ 1 & -4 & 1 \\ 0 & 1 & 0 \end{bmatrix}. \quad (7)$$

3.2 Experiments for Heat-diffusion IELs

In our experiments, we will evaluate the effectiveness of heat-diffusion IELs on semantic segmentation tasks using different datasets with both normal and noisy labels. We will use three well-known neural network architectures, namely Unet [25], DeepLab [6] and HRNetV2-W48 [28]. Table 3.2 provides the details on the number of IELs and Δt we adopt for each network. Our experiments demonstrate that the heat-diffusion IELs are particularly effective for datasets with noisy labels.

3.2.1 Unet with Heat-diffusion IELs on WBC

We conducted a performance comparison between Unet and Unet with IELs on a small dataset called the White Blood Cell (WBC) [32] dataset which consists of three hundred images. In the experiment, 270 samples were used for training and the remaining 30 samples were used

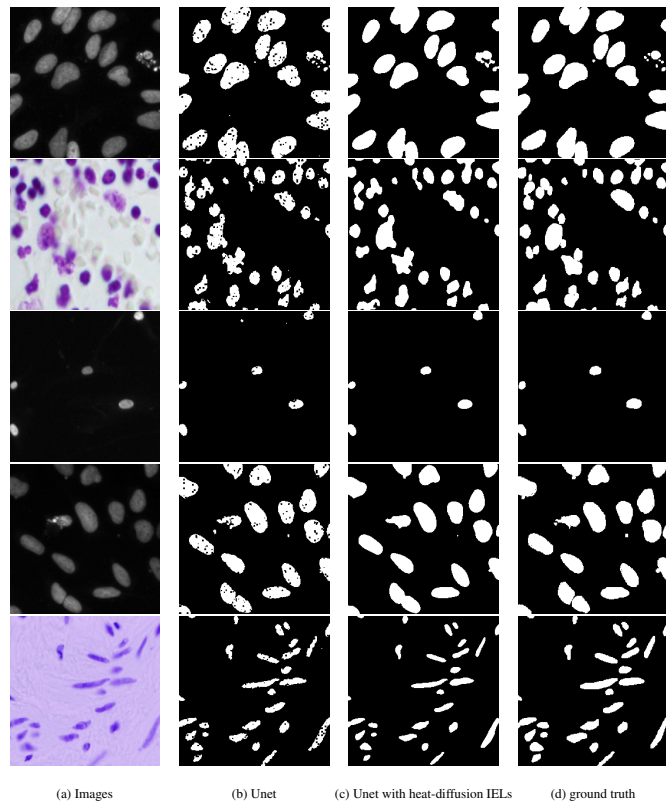


Figure 5: Comparison between Unet [25] and Unet with heat-diffusion IELs on 2018 Data Science Bowl dataset with noisy labels. (a) and (d) are the original images and the corresponding ground truth, respectively. (b) and (c) exhibit the segmentation results of the original Unet and Unet with heat-diffusion IELs, respectively.

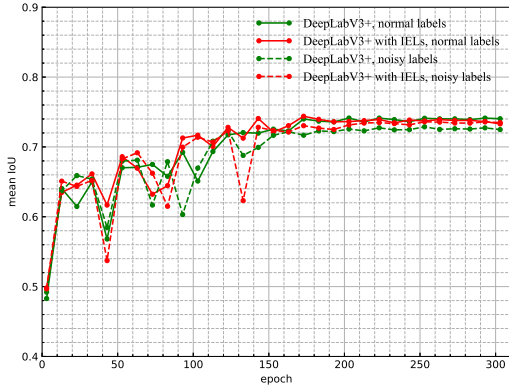


Figure 6: Mean IoU on the validation set of Cityscapes dataset based on DeepLabV3+ [6] and DeepLabV3+ with heat-diffusion IELs. The results of DeepLabV3+ and DeepLabV3+ with heat-diffusion IELs are highlighted by green lines and red lines, respectively. The results on normal labels and noisy labels are marked by solid lines and dotted lines, respectively.

for validation. The comparison is conducted on both normal and noisy labels. The way we add noise to training labels is to randomly choose some small windows on each label and replace their values with a random class. All noise windows in each label are 2×2 and the total area of the noise is set to 10 percent of the image size. The Unet structure used in the experiment has depth of 5 and the specific configuration in each level consists of 3×3 convolution layers, instance norm and leaky ReLu. Down-sampling and up-sampling are achieved by pooling operation and up-convolution, respectively. The total number of epochs is set to 20, with a learning rate of 0.0001. The loss function used is the cross-entropy loss.

The experimental results for the WBC dataset are presented in Figure 2 where the evaluation metric is the mean of dice score (DS) on the validation dataset. Segmentation results on noisy labels are displayed in Figure 3. Figure 2 shows that the original Unet and Unet with IELs have comparable performance on normal labels but Unet with IELs is much more robust to noisy labels. These results suggest that heat-diffusion IELs do not reduce the performance of the original Unet but rather significantly im-

prove it on noisy labels. In Figure 3, the results of the Unet are full of noise, which can be expected since neural networks are prone to the noise [31], while the segmentation maps of Unet with IELs have almost no noise. These results also indicate that the designed heat-diffusion IELs can act as regularizers and effectively prevent the Unet from overfitting noise.

3.2.2 Unet with Heat-diffusion IELs on 2018 Data Science Bowl

After the experiments on the WBC dataset, we extend the comparison to the 2018 Data Science Bowl dataset [3], which contains 607 training and 67 test images. In our experiment, the test images were used for validation during training. The comparison was also conducted on both normal labels and noisy labels. And the way we add noise is identical to that in the WBC dataset except that the size of noise windows is tuned to 3×3 . The comparison results are displayed in Figure 4 and Figure 5. Figure 4 shows that on the 2018 Data Science Bowl dataset, the heat-diffusion IELs can still maintain the performance of the Unet on normal labels and prevent the Unet from overfitting to noisy labels. As shown in the Figure 5, the original Unet still suffers a lot from noisy labels while Unet with IELs achieves much more satisfactory results on noisy labels.

3.2.3 DeepLabV3+ with Heat-diffusion IELs on Cityscapes

In addition to the datasets for medical images, we also evaluate the performance of our IELs on images obtained from real-world scenarios. The dataset we employ for the evaluation is the Cityscapes dataset [11] which contains 2795 train and 500 validation images and the corresponding neural networks we test on this dataset are the DeepLabV3+ [6] and HRNetV2-W48 [28]. The way we add noise is identical to the previous experiments except that the size of noise windows is 5×5 , which is also quite small compared to the image size (1024×2048).

For DeepLabV3+, we use ResNet-101 as the backbone and the results are presented in Figure 6, where the mean of class-wise intersection over union (mIoU) is adopted as the evaluation metric. These results indicate that for normal labels, DeepLabV3+ and its IELs

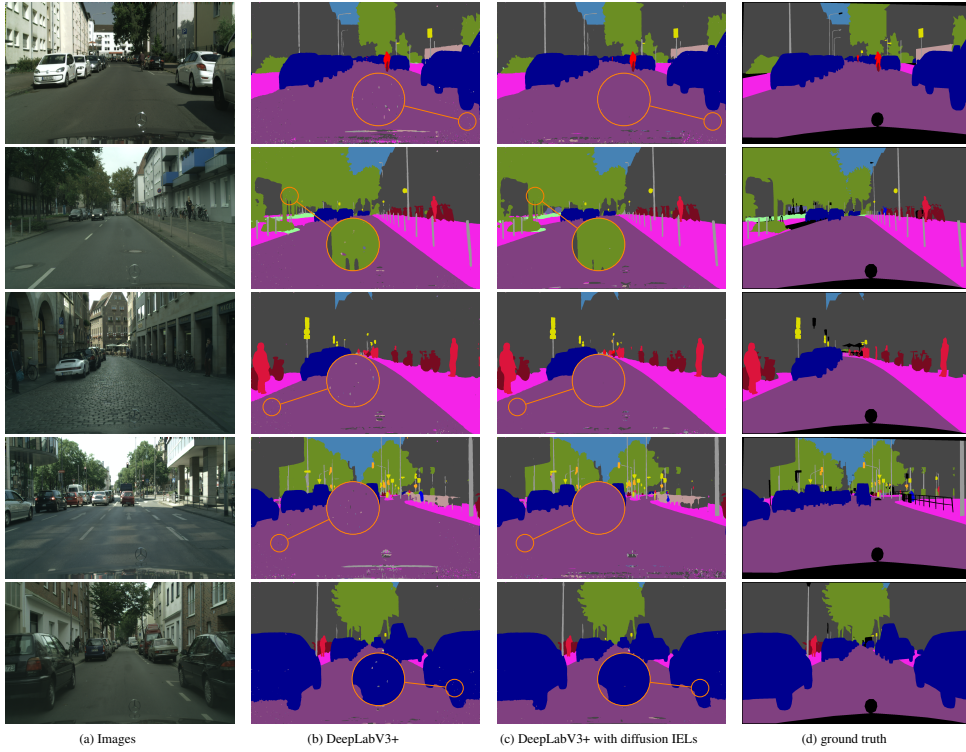


Figure 7: Comparison between DeepLabV3+ [6] and DeepLabV3+ with heat-diffusion IELs on Cityscapes dataset with noisy labels. (a) and (d) are the original images and the corresponding ground truth, respectively. (b) and (c) exhibit the segmentation results of the original DeepLabV3+ and DeepLabV3+ with heat-diffusion IELs, respectively. (The noise in (b) is not obvious since the noise size is quite small. Noise can be observed by zooming in on the four corners of these images.)

counterpart show similar performance while for noisy labels DeepLabV3+ with IELs outperforms the original DeepLabV3+. This demonstrate that IELs are effective in mitigating the impact of noise in labels. Furthermore, Figure 7 provides the detailed segmentation maps, which indicate that DeepLabV3+ tends to overfit the noise in labels whereas DeepLabV3+ with heat-diffusion IELs can generate accurate segmentation map with minimal noise.

3.2.4 HRNetV2-W48 with Heat-diffusion IELs on Cityscapes

Furthermore, we test the HRNetV2-W48 and its IELs counterpart on the Cityscapes dataset. To expedite the training process, a pretrained model is utilized. The results are displayed in Figure 8. We use the same evaluation metric, mIoU, for this experiment as well. While HRNetV2-W48 achieves high mIoU for the validation dataset, its tendency to overfit on noisy labels is more prominent than that of DeepLabV3+. This is due to the fact that HRNetV2-W48 relies heavily on the high-resolution features which are more susceptible to noise. Nevertheless, our heat-diffusion IELs significantly mitigate this overfitting, as evident from the results. Additionally, Figure 9 provides detailed segmentation maps, which further demonstrate the effectiveness of our heat-diffusion IELs in handling noise in labels.

4 Conclusion and Future Work

This paper proposes inverse evolution layers (IELs) as a regularization technique for neural networks. The aim of IELs is to guide the neural networks to produce outputs with expected partial differential equation (PDE) priors, thereby endowing them with appropriate properties. IELs can be easily incorporated into various neural networks without the introduction of new learnable parameters. Moreover, the integration of IELs does not compromise the learning ability of neural networks. We demonstrate the effectiveness of IELs through the use of heat-diffusion IELs to address the issue of noisy labels in semantic segmentation. Our experiments illustrate the efficacy of diffusion IELs in this regard. Overall, our proposed approach represents a remarkable contribution to the field of neural network regularization, offering a

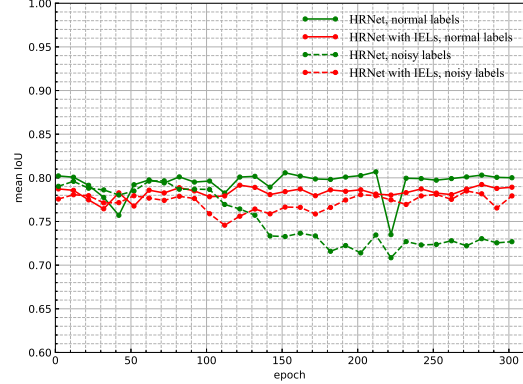


Figure 8: Mean IoU on the validation set of Cityscapes dataset based on HRNetV2-W48 [28] and HRNetV2-W48 with heat-diffusion IELs. The results of HRNetV2-W48 and HRNetV2-W48 with heat-diffusion IELs are highlighted by green lines and red lines, respectively. The results on normal labels and noisy labels are marked by solid lines and dotted lines, respectively.

promising means of integrating PDE-based mathematical models into neural networks in a transparent, interpretable, and effective manner.

Regarding future work, we envisage that, apart from heat-diffusion layers, a variety of other IELs could be formulated to equip neural networks with diverse mathematical or physical properties to address specific image processing tasks such as image inpainting, image generation, classification using noisy or mislabeled data, and others. Additionally, extending IELs to other research domains such as natural language processing and generative models presents a promising area for further investigation. Furthermore, we anticipate developing rigorous theorems to clarify the working principle of IELs, thus facilitating their use in practice.

References

[1] Luigi Ambrosio and Vincenzo Maria Tortorelli. “Approximation of functional depending on jumps by elliptic functional via t -convergence”. In: *Com-*

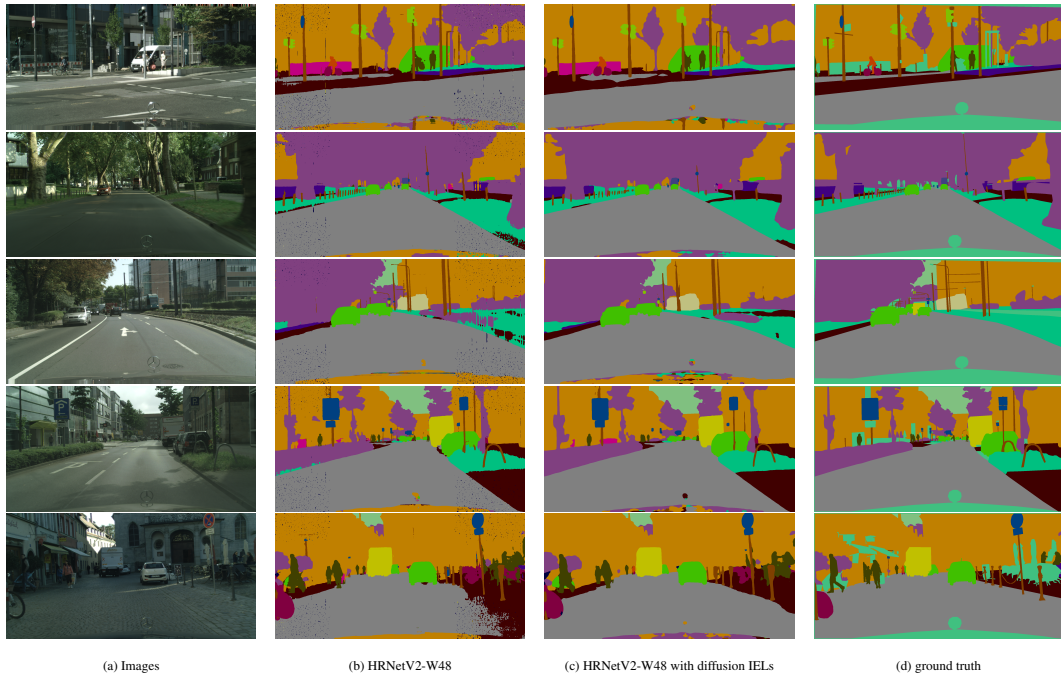


Figure 9: Comparison between HRNetV2-W48 [28] and HRNetV2-W48 with heat-diffusion IELs on Cityscapes dataset with noisy labels. (a) and (d) are the original images and the corresponding ground truth, respectively. (b) and (c) exhibit the segmentation results of the original HRNetV2-W48 and HRNetV2-W48 with heat-diffusion IELs, respectively.

munications on Pure and Applied Mathematics 43.8 (1990), pp. 999–1036.

[2] Vijay Badrinarayanan, Alex Kendall, and Roberto Cipolla. “Segnet: A deep convolutional encoder-decoder architecture for image segmentation”. In: *IEEE transactions on pattern analysis and machine intelligence* 39.12 (2017), pp. 2481–2495.

[3] Juan C Caicedo et al. “Nucleus segmentation across imaging experiments: the 2018 Data Science Bowl”. In: *Nature methods* 16.12 (2019), pp. 1247–1253.

[4] Nicolas Carion et al. “End-to-end object detection with transformers”. In: *Computer Vision–ECCV 2020: 16th European Conference, Glasgow, UK, August 23–28, 2020, Proceedings, Part I 16*. Springer. 2020, pp. 213–229.

[5] Tony F Chan and Luminita A Vese. “Active contours without edges”. In: *IEEE Transactions on image processing* 10.2 (2001), pp. 266–277.

[6] Liang-Chieh Chen et al. “Encoder-decoder with atrous separable convolution for semantic image segmentation”. In: *Proceedings of the European conference on computer vision (ECCV)*. 2018, pp. 801–818.

[7] Ricky TQ Chen et al. “Neural ordinary differential equations”. In: *Advances in neural information processing systems* 31 (2018).

[8] Xu Chen et al. “Learning active contour models for medical image segmentation”. In: *Proceedings of the IEEE/CVF conference on computer vision and pattern recognition*. 2019, pp. 11632–11640.

[9] Yunjin Chen, Wei Yu, and Thomas Pock. “On learning optimized reaction diffusion processes for effective image restoration”. In: *Proceedings of the IEEE conference on computer vision and pattern recognition*. 2015, pp. 5261–5269.

[10] Dominic Cheng et al. “Darnet: Deep active ray network for building segmentation”. In: *Proceedings of the IEEE/CVF Conference on Computer Vision and Pattern Recognition*. 2019, pp. 7431–7439.

[11] Marius Cordts et al. “The cityscapes dataset for semantic urban scene understanding”. In: *Proceedings of the IEEE conference on computer vision and pattern recognition*. 2016, pp. 3213–3223.

[12] Alexey Dosovitskiy et al. “An image is worth 16x16 words: Transformers for image recognition at scale”. In: *arXiv preprint arXiv:2010.11929* (2020).

[13] Ali Hatamizadeh, Debleena Sengupta, and Demetri Terzopoulos. “End-to-end deep convolutional active contours for image segmentation”. In: *arXiv preprint arXiv:1909.13359* (2019).

[14] Kaiming He et al. “Deep residual learning for image recognition”. In: *Proceedings of the IEEE conference on computer vision and pattern recognition*. 2016, pp. 770–778.

[15] Fabian Isensee et al. “nnU-Net: a self-configuring method for deep learning-based biomedical image segmentation”. In: *Nature methods* 18.2 (2021), pp. 203–211.

[16] Chaoyu Liu, Zhonghua Qiao, and Qian Zhang. “Two-Phase Segmentation for Intensity Inhomogeneous Images by the Allen–Cahn Local Binary Fitting Model”. In: *SIAM Journal on Scientific Computing* 44.1 (2022), B177–B196.

[17] Jun Liu, Xiangyue Wang, and Xue-cheng Tai. “Deep Convolutional Neural Networks with Spatial Regularization, Volume and Star-Shape Priors for Image Segmentation”. In: *Journal of Mathematical Imaging and Vision* (2022), pp. 1–21.

[18] Yiping Lu et al. “Beyond finite layer neural networks: Bridging deep architectures and numerical differential equations”. In: *International Conference on Machine Learning*. PMLR. 2018, pp. 3276–3285.

[19] Sebastian Lunz, Ozan Öktem, and Carola-Bibiane Schönlieb. “Adversarial regularizers in inverse problems”. In: *Advances in neural information processing systems* 31 (2018).

[20] Diego Marcos et al. “Learning deep structured active contours end-to-end”. In: *Proceedings of the IEEE Conference on Computer Vision and Pattern Recognition*. 2018, pp. 8877–8885.

- [21] David Bryant Mumford and Jayant Shah. “Optimal approximations by piecewise smooth functions and associated variational problems”. In: *Communications on pure and applied mathematics* (1989).
- [22] K Niklas Nordström. “Biased anisotropic diffusion: a unified regularization and diffusion approach to edge detection”. In: *Image and vision computing* 8.4 (1990), pp. 318–327.
- [23] Pietro Perona and Jitendra Malik. “Scale-space and edge detection using anisotropic diffusion”. In: *IEEE Transactions on pattern analysis and machine intelligence* 12.7 (1990), pp. 629–639.
- [24] Maziar Raissi, Paris Perdikaris, and George E Karniadakis. “Physics-informed neural networks: A deep learning framework for solving forward and inverse problems involving nonlinear partial differential equations”. In: *Journal of Computational physics* 378 (2019), pp. 686–707.
- [25] Olaf Ronneberger, Philipp Fischer, and Thomas Brox. “U-net: Convolutional networks for biomedical image segmentation”. In: *Medical Image Computing and Computer-Assisted Intervention—MICCAI 2015: 18th International Conference, Munich, Germany, October 5–9, 2015, Proceedings, Part III* 18. Springer. 2015, pp. 234–241.
- [26] Leonid I Rudin, Stanley Osher, and Emad Fatemi. “Nonlinear total variation based noise removal algorithms”. In: *Physica D: nonlinear phenomena* 60.1-4 (1992), pp. 259–268.
- [27] Lars Ruthotto and Eldad Haber. “Deep neural networks motivated by partial differential equations”. In: *Journal of Mathematical Imaging and Vision* 62.3 (2020), pp. 352–364.
- [28] Ke Sun et al. “High-resolution representations for labeling pixels and regions”. In: *arXiv preprint arXiv:1904.04514* (2019).
- [29] Joachim Weickert et al. *Anisotropic diffusion in image processing*. Vol. 1. Teubner Stuttgart, 1998.
- [30] E Weinan. “A proposal on machine learning via dynamical systems”. In: *Communications in Mathematics and Statistics* 1.5 (2017), pp. 1–11.
- [31] Chiyuan Zhang et al. “Understanding deep learning (still) requires rethinking generalization”. In: *Communications of the ACM* 64.3 (2021), pp. 107–115.
- [32] Xin Zheng et al. “Fast and robust segmentation of white blood cell images by self-supervised learning”. In: *Micron* 107 (2018), pp. 55–71.